Int. J. Heat Mass Transfer. Vol. 13, pp. 945–956. Pergamon Press 1970. Printed in Great Britain

DIRECT CONTACT HEAT TRANSFER WITH CHANGE OF PHASE

EVAPORATION OF DISCRETE VOLATILE FILMS FROM THE SURFACE OF A STAGNANT IMMISCIBLE LIQUID

M. BENTWICH†, U. LANDAU‡ and S. SIDEMAN

Technion—Israel of Technology, Haifa, Israel

(*Received* 19 *September* 1968 *and in revised form* 7 *January* 1969)

Abstract—The transfer efficiency of spray columns and other three phase exchangers, in which volatile matter evaporates (or condenses) while submerged in the non-volatile phase, is adversely affected by the hydrostatic head. This undesirable effect on the temperature driving force may be overcome by utilizing systems in which the evaporating matter is allowed to float on an immiscible non-volatile liquid. This work is a first attempt to test the practicality of such an exchanger. Lower bound values of the heat-transfer coefficients are obtained from a quasi-steady state solution for an evaporating lens-shaped drop placed on a semi-infinite stagnant liquid medium.

Experimental work confirms the theoretical prediction that the rate of change of the radius of the lens with time is a ΔT dependent constant. However, the measured evaporation rates, hence the transfer coefficients, are found larger than those calculated. This is taken as an indication that interfacial convection plays an important role in processes of this type even at low temperature driving forces. The experimental transfer coefficients obtained in this work, compare favourably with those reported in the literature for evaporation of volatile liquids in disperions.

NOMENCLATURE

A, area of contact, equation (30);
a, constant, equations (20), (27);
A_n, coefficient in the expansion (8);
b, exponent, equation (20);
B_n, coefficient in the expansion (9);
D, instantaneous diameter of lens;
D_i, initial diameter of lens;
D_s, equivalent spherical diameter;
g, gravitational acceleration;
$h_\xi h_\eta h_\zeta$, diagonal components of metric tensor;
h, instantaneous heat-transfer coefficient, theoretical;
h_e, instantaneous heat-transfer coefficient, experimental [cal/s °C cm^2];
$\bar{h}$, time averaged heat-transfer coefficient [cal/s °C cm^2];
$\bar{h}_e$, time averaged heat-transfer coefficient, experimental [cal/s °C cm^2];
$\bar{h}_i$, ditto, related to initial area of spherical drop [cal/s °C cm^2];
k, coefficient of thermal conductivity [cal/s °C cm];
L, latent heat, volumetric [cal/s °C cm];
l, thickness of lens [mm];
m, slope of (dR/dt) vs. ΔT curve obtained from experiment;
m_t, slope of (dR/dt) vs. ΔT curve obtained theoretically;
n, running index; integer;
Nu, Nusselt number, $= 2Rh/k$;
$\overline{Nu}$, Nusselt number, time averaged $= 2R_i\bar{h}/k$;
$P_n(\mu)$, Legendre polynomial of the first kind of degree n and argument μ;
q, local heat flux;

† Present address: Department of Mechanics, College of Engineering, State University of New York at Stony Brook, Stony Brook, New York.

‡ Present address: Mechanical Engineering Department, Berkeley, California.

$Q_n(iv)$; Legendre polynomial of the second kind of degree n and argument iv;
r, radial coordinate;
R, instantaneous radius (of lens or film);
R_i, initial radius (or lens or film) [cm];
S', spreading coefficient for saturated system [dyn/cm];
t, time variable [s];
$\hat{t}$, time of evaporation of 95 per cent of the initial volume;
T_0, temperature [°C];
T_b, bulk temperature [°C];
T, temperature of volatile film [°C];
T_∞, undisturbed temperature field at infinity;
V, volume of drop or film [cm^3];
z, axial coordinate.

Greek letters

β, ratio of conductivities;
ξ, η, ellipsoidal coordinates, Fig. 2;
$\hat{\xi}$, value of ξ at the pentane–water interface;
θ, polar angle;
ζ, ellipsoidal coordinate;
$\hat{\nu}$, value of ν at the pentane–water interface;
ρ, fluid density [g/cm^3];
σ, surface tension;
ν, μ, transformation variables.

Subscripts

b, bulk;
e, experimental;
i, initial radius, diameter or area;
p, pentane;
s, spherical;
w, water;
∞, infinity.

INTRODUCTION

THE QUEST for economic desalination units has recently stimulated research in the field of direct contact heat transfer with change of phase. This relatively new mode of heat transfer is particularly promising for processes in which the temperature driving forces are very small and/or heat recovery is of paramount economic importance. An efficient multiphase exchanger utilizing latent, rather than sensible, heat transfer is obviously the ultimate goal of these studies.

Previous work on three-phase exchangers and freezers utilizing a secondary refrigerant [1] is based on evaporation of the volatile liquid while in dispersion in the continuous immiscible liquid phase. This mode of operation is aimed at large interfacial contact areas per unit equipment volume. However, detailed studies of the mechanism of heat transfer in single and multi-drop systems [2–4] showed that the transfer efficiency is negatively affected by the hydrostatic head. A water head of some 50 cm effects an increase of the boiling point by roughly 1°C. It therefore reduces the effective driving force by the same amount. This, of course, is particularly pronounced at low temperature driving forces (1–2°C) which are presently of practical importance.

Evaporation of drops in shallow layers of the continuous immiscible liquid will clearly overcome the limitation imposed by the hydrostatic head. However, only partial evaporation will occur under these conditions and the unevaporated liquid will then form a finite film on the surface of the immiscible liquid. These films may remain discrete (as lens of finite-size films) or else coalesce and form a continuous film over the surface. A basic study of evaporation of such films is, therefore, called for. By utilizing films rather than, or in conjecture with, dispersions, a better and more efficient multiphase exchanger is anticipated.

In this preliminary research the authors study experimentally and theoretically a lens, or a film, floating on a large expanse of immiscible liquid. The purpose of this work is to compare the measured values of the overall heat-transfer rate with theoretical estimations of this quantity.

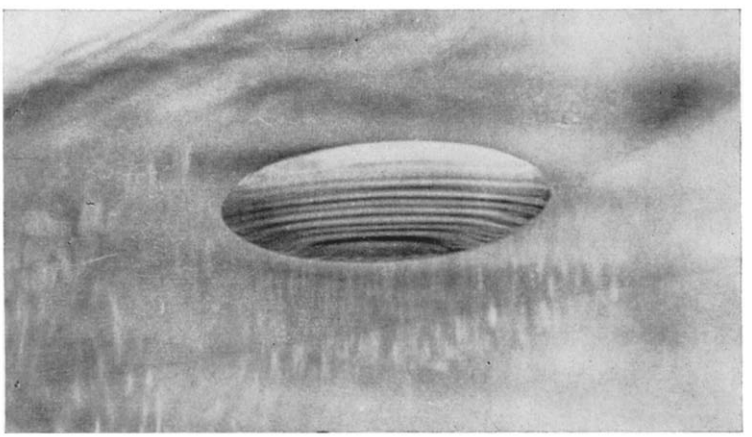

FIG. 1. Isopentane lens on water.

[*facing page* 946]

In the experimental set-up and in the analysis the evaporation is controlled by the heat transfer. This is insured by letting the volatile film evaporate into a confined, practically saturated, atmosphere. (The newly generated vapors are sucked out of the system by keeping the condenser at a somewhat lower pressure.) The exposed surface is thus maintained at the corresponding boiling temperature. The prevailing temperatures and temperature gradients are low so that radiation effects are negligible. It is further assumed that the interface and the films are stable (see Fig. 1).

A rough calculation of the heat-transfer rate is carried out assuming that the lens is rotationally symmetric and ellipsoidal. First, a general expression for the steady temperature distribution in the convection-free two phase system is constructed. It contains a parameter β, the ratio of the conductivity of the pentane to that of water. It is then shown that for the appropriate ellipsoidal axes-ratio the temperature distribution in the lens is essentially uniform unless β is $0(10^{-3})$ or smaller. For the pentane–water system β is about $\frac{1}{3}$ so that the temperature drop through the volatile liquid is negligible. Unfortunately, this analysis does not take into account convection currents due to cooling on top which tend to increase the transfer in the non-volatile liquid. However, it is unlikely that the increase in the transfer due to that effect would be equivalent to 100-fold increase in the conductivity of the non volatile liquid. Indeed the correlation with the experimental results suggests that the mathematical model yields total transfer rates which can serve as a meaningful lower bounds to those measured. The transfer rates are calculated by interpreting the solution for the temperatures distribution as a quasi-steady one. Accordingly the transfer at any instant is assumed to be unaffected by the contraction of the lens.

MATHEMATICAL ANALYSIS

As explained, solution is obtained for the steady temperature distribution T in the purely conductive two phase system shown in Fig. 2. In view of the assumed geometry of the lens oblate spheroidal co-ordinates are used here. These are related to the cylindrical co-ordinates (r, θ, z) in the following manner

$$r = R\cosh\xi\cosh\eta \quad z = R\sinh\xi\sin\eta \quad \theta = \zeta. \tag{1}$$

In terms of these the diagonal components of the metric tensor are

$$h_\xi^2 = h_\eta^2 = R^2(\cosh^2\xi - \cos^2\eta)$$
$$h_\zeta^2 = R^2\cosh^2\xi\cos^2\eta. \tag{2}$$

The interface is defined by

$$\xi = \hat{\xi}, \quad -\pi/2 < \eta < 0.$$

A solution for T is sought which satisfies

$$0 = \nabla^2 T = R^{-2}(\cosh^2\xi - \cos^2\eta)^{-1} \times \left[\frac{1}{\cosh\xi}\frac{\partial}{\partial\xi}\cosh\xi\frac{\partial}{\partial\xi} + \frac{1}{\cos\eta}\frac{\partial}{\partial\eta}\cos\eta\frac{\partial}{\partial\eta}\right]T \tag{3}$$

in each phase and for which the temperature and the heat-flux are continuous across the interface.

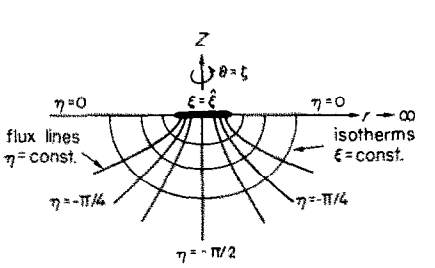

FIG. 2. Schematic presentation of coordinates.

The boundary conditions for the problem are

$$T = T_0 \quad \xi = \hat{\xi}, \quad 0 < \eta < \pi/2, \tag{4}$$

$$T \to T_\infty \quad \xi \to \infty, \quad -\pi/2 < \eta < 0, \tag{5}$$

$$\partial T/\partial\eta = 0 \quad \xi > \hat{\xi}, \quad \eta = 0. \tag{6}$$

Condition (5) is in line with the assumptions made in the Introduction. T_∞ is the temperature

of the non-volatile liquid. Equation (6) implies that no heat transfer takes place between this liquid and the adjacent atmosphere.

It can be easily shown that the method of separation of variables yields solutions in terms of Legendre Polynomials P_n and related functions Q_n. The general solution for T in each phase is

$$T = T_\infty + (T_0 - T_\infty)\sum_{n=0}^{\infty} A_n \frac{P_n(iv)}{P_n(i\hat{v})} P_n(\mu) \qquad v < \hat{v}, \quad -1 < \mu < 1 \tag{8}$$

$$T = T_\infty + (T_0 - T_\infty)\sum_{k=0}^{\infty} B_{2k} \frac{Q_{2k}(iv)}{Q_{2k}(i\hat{v})} P_{2k}(\mu) \qquad \hat{v} < v, \quad -1 < \mu < 0 \tag{9}$$

where

$$\mu = \sin\eta \qquad v = \sinh\xi \qquad \hat{v} = \sinh\hat{\xi}. \tag{10}$$

In view of the condition (6) the second expansion includes only even terms. The dependence on v is given by Q_{2k} for the outer domain so as to satisfy condition (5). The functions Q_n do not appear in equation (8) because these give rise to a discontinuous derivative along $v = 0$.

By matching the two expressions for the temperature and the flux at the interface one gets equalities between two infinite series. Since within the range $-1 < \mu < 0$ the P_{2k} constitutes a complete orthogonal series these two requirements reduce to [5, 6].

$$\sum_{m=0}^{\infty}\left(\int_{-1}^{0} P_{2m+1} P_{2j}\,\mathrm{d}\mu\right) A_{2m+1} + \left(\int_{-1}^{0} P_{2j}^2\,\mathrm{d}\mu\right)(A_{2j} - B_{2j}) = 0 \tag{11j}$$

$$\beta\sum_{m=0}^{\infty}\frac{P'_{2m+1}(i\hat{v})}{P_{2m+1}(i\hat{v})}\left(\int_{-1}^{0} P_{2m+1} P_{2j}\,\mathrm{d}\mu\right) A_{2m+1} + \left(\beta\frac{P'_{2j}(i\hat{v})}{P_{2j}(i\hat{v})}A_{2j} - \frac{Q'_{2j}(i\hat{v})}{Q_{2j}(i\hat{v})}B_{2j}\right) \times\left(\int_{-1}^{0} P_{2j}^2\,\mathrm{d}\mu\right) = 0. \tag{12j}$$

Since P_{2k} have the same properties in the range $0 < \mu < 1$ equation (4) reduces to

$$\left(\int_{0}^{1} P_{2j}^2\,\mathrm{d}\mu\right) A_{2j} + \sum_{m=0}^{\infty}\left(\int_{0}^{1} P_{2m+1} P_{2j}\,\mathrm{d}\mu\right) A_{2m+1} = \delta_{j0} \tag{13j}$$

where δ_{ij} is Kroneker delta. By setting equations (11j), (12j) and (13j) for $j = 0, 1, 2, \ldots, (\tilde{j} - 1)$ one can solve for $A_0, A_1, \ldots, A_{2j-1}, B_0, B_2, \ldots, B_{2j-2}$, assuming that all other coefficients vanish. Since the series (8) and (9) converge the truncation error can be diminished by increasing $\tilde{j}$.

APPLICATION OF THE MODEL

Though this analysis holds for any value of β and ellipsoidal axes ratio $\hat{v}(1 + \hat{v}^2)^{-\frac{1}{2}}$, attention is now focused on the case in which $\hat{v}$ is extremely small. By combining linearly equations (11j) (12j) one can eliminate B_{2j} and get:

$$\sum_{m=0}^{\infty}\{\beta P'_{2m+1}(i\hat{v})/P_{2m+1}(i\hat{v}) - Q'_{2j}(i\hat{v})/Q_{2j}(i\hat{v})\} \times\left(\int_{-1}^{0} P_{2m+1}P_{2j}\,\mathrm{d}\mu\right) A_{2m+1} + \{\beta P'_{2j}(i\hat{v})/P_{ij}(i\hat{v}) - Q'_{2j}(i\hat{v})/Q_{ij}(i\hat{v})\}\left(\int_{-1}^{0} P_{2j}^2\,\mathrm{d}\mu\right) A_{2j} = 0. \tag{14j}$$

The multipliers in curly brackets contain the terms $\beta P'_n(i\hat{v})/P_n(i\hat{v})$ which are of $O(\beta/\hat{v})$ for $n \neq 0$. It therefore follows from equation (14j) that the coefficients A_{2m+1} are smaller from A_0 by a factor of $O(\hat{v}/\beta)$. Consequently, in view of equations (13_0) and (11_0) one gets the result

$$A_0 = 1 + O(\hat{v}/\beta) \qquad B_0 = 1 + O(\hat{v}/\beta). \tag{15}$$

Since $\hat{v}$ is $0(10^{-2})$ the last two relationships are taken to be sufficiently accurate.

Under the assumption of quasi-steady state, the instantaneous heat flux required to maintain the evaporation is

$$q = k[h_\xi^{-1}(\partial T/\partial\xi)]_{\xi=\hat{\xi}}. \tag{16}$$

Using equations (8) and (16) and choosing the logarithmic branch in the expression for Q_0

so that the following holds

$$Q_0(i\hat{v}) = -\pi/2 + 0(\hat{v})$$

one finds that the heat transfer over the entire interface, Q, is given by

$$Q = k \int_0^{2\pi} \int_0^{\pi/2} [h_\xi^{-1}(\partial T/\partial \xi)]\, h_\zeta h_\eta \, d\eta \, d\zeta = -4k\, R(T_0 - T_\infty) + 0(\hat{v}). \quad (17)$$

The error involved in equation (17) is negligible. Equation (17) is identical with the solution obtained [7] for heating a semi-infinite body by a constant temperature disk like heat source, using the discontinuous properties of a Bessel function integral, which happen to satisfy the required boundary condition.

The instantaneous heat-transfer rate associated with the continuous contraction of the volume V of the extended volatile mass is given by

$$Q = L(dV/dt) \quad (18)$$

where L is the volumetric latent heat of evaporation of the volatile lighter fluid. The combination of equations (17) and (18) yields:

$$(dV/dt) = -4kR(T_\infty - T_0)/L. \quad (19)$$

Obviously, the quantities V and R are interdependent and can be related quite generally by

$$V = ak^b \qquad 2 \leqslant b \leqslant 3 \quad (20)$$

where a is a constant, dependent on the value of b. The upper limit $b = 3$ corresponds to the case where the average thickness of the liquid lens is proportional to the radius, as in a spherical drop, for instance. The lower limit $b = 2$ corresponds to a process in which the average thickness of the liquid film or lens remains constant throughout. Evidently, the latter condition is appropriate for extended films, whereas the former may probably be applicable to a very small lens (at the end of the process). For $b = 3$, equation (19) reduces to

$$d(\pi R^2)/dt = -(2k/L)(T_\infty - T_0) \quad (21)$$

implying that for a given temperature driving force the rate of area change will be constant. For $b = 2$, equation (19) reduces to

$$dR/dt = -(2k/aL)(T_\infty - T_0) \quad (22)$$

indicating that for extended masses the radius contracts uniformly with time.

Finally, it is interesting to note that the instantaneous heat-transfer coefficient h (related to the instantaneous area) is equal to

$$h \equiv \frac{Q}{(T_0 - T_\infty)\pi R^2} \equiv \frac{4k}{\pi R} \quad (23)$$

and the Nusselt number is given by

$$Nu = 2Rh/k = 8/\pi = 2{\cdot}54. \quad (24)$$

The last relationship indicates that for a continuously replenished film, the lower bound Nu number is constant. Its value is higher than the value of 2·0 calculated for diffusion from a stagnant sphere.

The heat-transfer coefficient, $\bar{h}$, averaged over $\hat{t}$, the time of evaporation of 95 per cent of the initial volume (or about 90 per cent of the initial radius R_i) is given by

$$\bar{h} = \frac{1}{\hat{t}} \int_0^{\hat{t}} h(t)\, dt = -\frac{1}{0{\cdot}9\, R_i} \int_{R_i}^{0{\cdot}1R_i} \frac{4k}{\pi R}\, dR = 3{\cdot}26k/R_i \quad (25)$$

since $(dR/dt) =$ constant. The time averaged Nusselt number, related to the initial radius, is

$$\overline{Nu} = 2R_i\bar{h}/k = 6{\cdot}51. \quad (26)$$

(If $\bar{h}$ is calculated for the time corresponding to the evaporation of 99 per cent R_i, then $\bar{h} = 18{\cdot}4\, k/\pi R_i$ and $\overline{Nu} = 36{\cdot}8/\pi$.)

EXPERIMENTAL

Isopentane and distilled water were chosen for this study. This system allows for convenient work and is closely related to the foreseen practical systems [2, 4]. Schematic diagram of the apparatus is presented in Fig. 3(a).

The evaporation chamber, Fig. 3(b), was a square 12·5 × 12·5 cm, 30 cm high, hermetically sealed at the top and bottom by Perspex sheets. The water height inside was 23 cm, leaving

a vapor volume of approximately one litre. The water was kept at a constant temperature, by means of an immersed electric heater, controlled by a Jumo contact Thermometer, and a magnetic stirrer. The interface could be rejuvenated by means of a variable height overflow. This allowed to maintain a clean interface for each run.

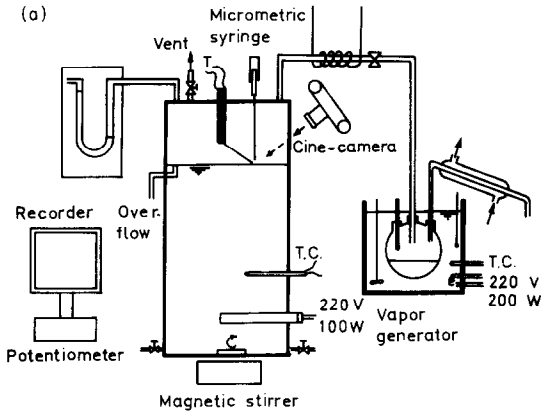

FIG. 3(a). Schematic diagram of apparatus.

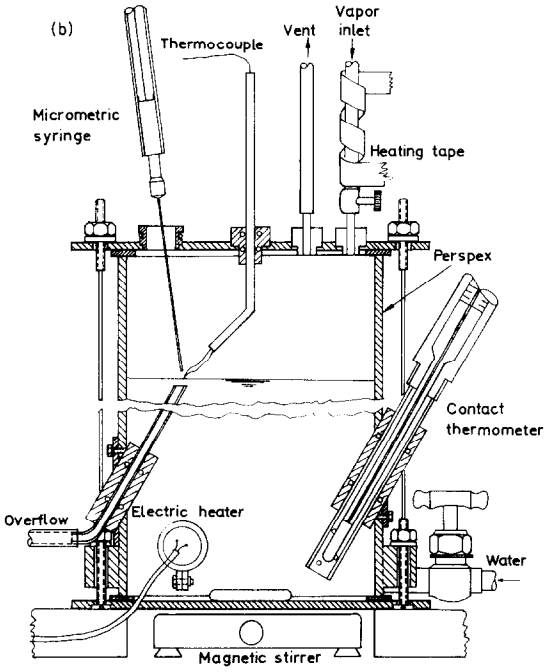

FIG. 3(b). Evaporation chamber.

An isopentane vapor generator, connected to the upper part of the chamber, supplied a continuous flow of saturated vapor into the vapor space. In order to avoid excess condensation, the connecting line was slightly heated by means of an electric heating tape. A water U-tube manometer was used to determine the pressure in the chamber.

The isopentane lens was obtained by injecting isopentane drops through an hypodermic needle, connected to an Agla micrometric syringe, situated some 2-mm above the water surface.

The lens temperature during the evaporation process could be recorded by means of a fine, S.W.G. 50, copper–constantan thermocouple with a 0·1 mm junction, imbedded in the isopentane lens, and connected to a fast, 8 in./min, Servoriter II (Texas Instruments) recorder. The insertion of the thermocouple's junction into the lens could be controlled by manipulating the water level with the aid of a fine needle valve. The same thermocouple was used to measure the water bulk temperature before and after each run. The room temperature was kept constant 0·5°C ($\pm$0·1) above the isopentane normal boiling point, thus avoiding condensation of isopentane on the Perspex walls.

The evaporating lenses were photographed with a Paillard Bolex H-16 Reflex cine-camera, at 11·5 ft/s. Best results were obtained using a 150 mm telescopic Macro Yvar lens, with a 75 mm extension tube, and back lighting through an horizontal grid [8].

Particular care was taken to prevent the presence of air. This was accomplished by displacing the initially water-filler slowly with isopentane vapor. Traces of air could be detected by an appreciable decrease in the recorded evaporation temperature. Also, the recorded temperature history of the lens provided a check on the final evaporation time.

In order to keep the water surface stable and

the lens stationary, the stirrer was shut off for 3 min before each run.

EXPERIMENTAL RESULTS

1. *The characteristic shape and thickness of the evaporating lens*

The actual relationship between the volume of the lens and its diameter was experimentally determined by direct measurements of the pictures of the evaporating lenses. The initial volume was taken as that of the falling spherical drop from which the lens was formed. Plotting these volumes vs. the initial lenses' diameter (not shown here) yielded the following relationship:

$$V = (8{\cdot}07) \times 10^{-3} D^{2{\cdot}016} \simeq (3{\cdot}2) \times 10^{-2} R^2 \tag{27}$$

which is based on a least square calculation of some 50 drops, with volumes ranging from 2 to 40 mm^3. Equation (27) substantiates the theoretical relationship given by equation (20) with $a = 3{\cdot}2 \times 10^{-2}$ cm and $b = 2$, i.e. for constant thickness lenses. By assuming the lens to be an oblate spheroid, the thickness of the isopentane lenses was calculated to be 0·15 mm.

For comparison, the constant thickness of larger lense (4–6 cm in diameter) was also calculated using Langmuir's [9] expressions based on interfacial tensions:

$$l = \left(- \frac{2S'\rho_w}{g\rho_p(\rho_w - \rho_p)} \right)^{0{\cdot}5} \tag{28}$$

where S', the spreading coefficient, is given by

$$S' = \sigma'_w - \sigma'_p - \sigma'_{wp} = -0{\cdot}04$$

and g, ρ_w, ρ_p denote the gravitational acceleration, and the densities of water and (liquid) isopentane, respectively. The experimentally determined surface tension of water saturated with isopentane, σ'_w, is 62·63 dyn/cm. The value for isopentane saturated with water, σ'_p, is 13·04 dyn/cm, and σ'_{wp}, the interfacial water–pentane surface tension for the mutually saturated liquids is 49·62 dyn/cm. These values were obtained at 22°C using a ring ballance tensiomer. Equation (28) yields $l = 0{\cdot}18$ mm. Considering the lens' shape assumed here as compared with Langmuir's and the possibility of some error in the experimental values of the surface tension, the agreement is quite satisfactory.

It should be stated that the isopentane lens

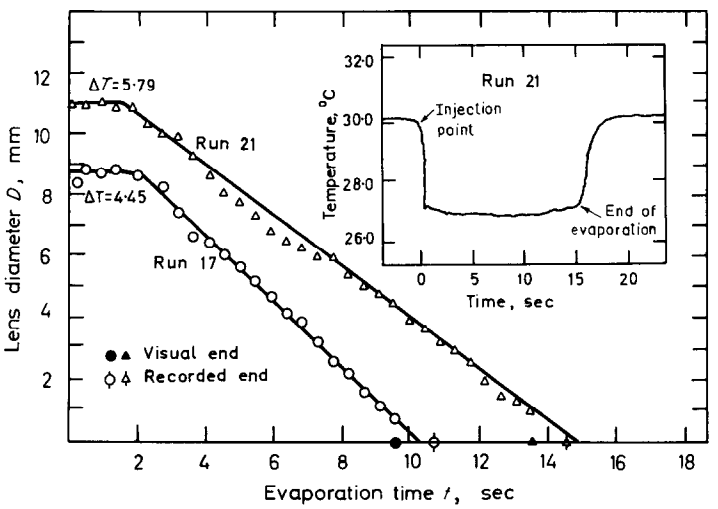

FIG. 4. Representative diameter vs. time curves.

will form only on an isopentane saturated water surface. Should this interface be unsaturated, a positive spreading sufficient will cause the isopentane drop to spread and form a very thin film on the interface. Thus, all the work presented here was carried out on pentane-saturated interfaces.

2. *Evaporation rate*

A typical plot representing the evaporation process is presented in Fig. 4. The data were obtained by direct measurements of the projected frames of the film taken of the evaporating lens. Also included in Fig. 4 is the recorded temperature history of the representative lens. The experimental results show that over most of the vaporization process, the diameter decreases linearly with time, as predicted by equation (22). Within the experimental accuracy, no evaporation takes place during the initial period of lens formation. In this period the forming lens is seen to spread and contract until it stabilizes. The time dependency of the lens' diameter beyond the linear region is somewhat less certain. The exact time of complete evaporation may depend either on visual observation or else on the response of the embedded thermocouple. As shown in Fig. 4, these two readings do not coincide, thus leaving the question of evaporation rates of very small lens ($< 0{\cdot}5$ mm) still unresolved. As stated in the theoretical part, it is, however, reasonable to assume that in this narrow size range the area rather than the diameter would vary linearly with time.

As shown in Fig. 5, the time rate of change of the radius is independent of the radius and is a linear function of the temperature driving force, i.e.

$$\frac{dR}{dt} = -m(T_b - T_0)$$

where T_b is the water bulk temperature and T_0 is the boiling point temperature corresponding the partial isopentane vapor pressure. A least-square calculation for all the lenses, going through the origin, yields $m = 6{\cdot}4 \times 10^{-3}$ cm/s °C, as compared with the value given by equation (22) whereby $m_t = 2k/aL = 1{\cdot}82 \times 10^{-3}$ cm/s °C.

3. *The heat-transfer coefficient*

The experimental instantaneous values can be calculated making use of equation (27) for

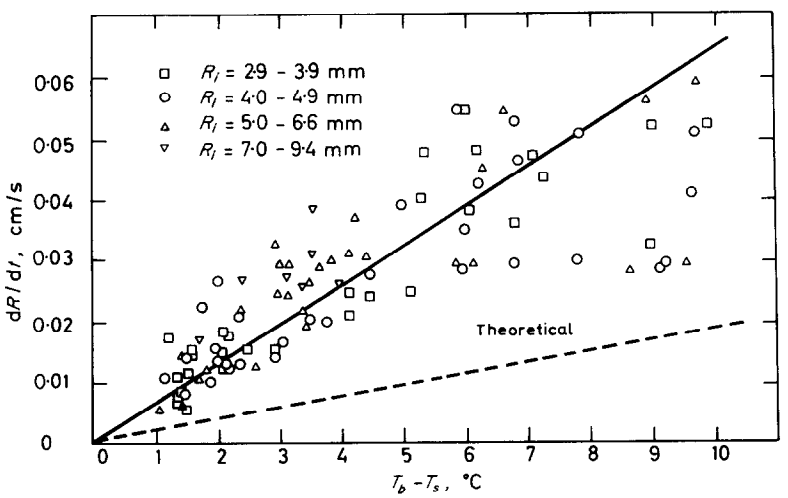

FIG. 5. Rate of change of radius vs. temperature driving force.

each lens, by the following relationships:

$$h_e = \frac{Q}{A\,\Delta T} = \frac{L}{A\,\Delta T}\,\frac{dV}{dt} = \frac{2aL}{R\,\Delta T}\,\frac{dR}{dt}.$$

However, a more general, and undoubtedly more reliable value is obtained by utilizing equation (29). Equation (30) then reduces to

$$h_l = \frac{2aLm}{\pi R} = \frac{6{\cdot}6 \times 10^{-3}}{R}$$

where h_e is given in cal/s cm^2 °C.

The time averaged experimental heat transfer coefficients were calculated for $\hat{t}$, the time in

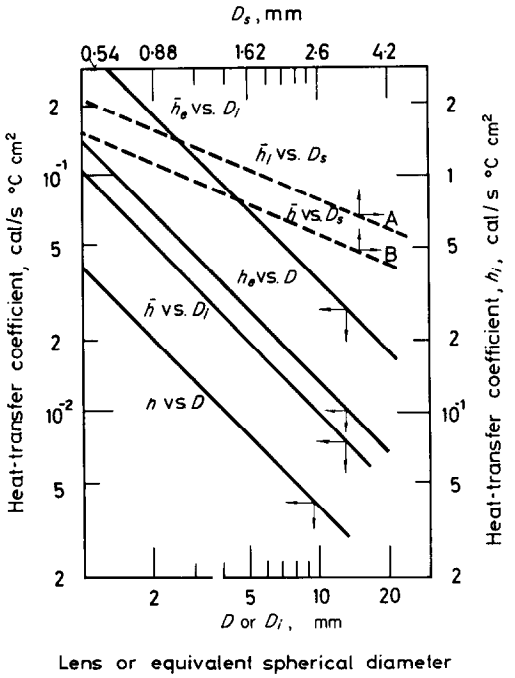

FIG. 6. Instantaneous and average heat transfer coefficients as function of lens or drop diameter.

which 90 per cent of the initial radius disappears, by

$$\bar{h}_e = \frac{1}{\hat{t}}\int_0^{\hat{t}} h_e\,dt = \frac{1}{0{\cdot}9R_i}\int_{R_i}^{0{\cdot}1R_i} h_e\,dR$$

$$= 1{\cdot}63\,\frac{amL}{R_i} = \frac{1{\cdot}69 \times 10^{-2}}{R_i}.$$

A comparison of the experimental heat-transfer coefficients with the lower bound value predicted theoretically by equations (23) and (25) is given in Fig. 6.

DISCUSSION

The experiments presented substantiate the theoretically predicted functional relationships. The linear relationship of the contracting radius with time is associated with a constant thickness lens. This characteristic was verified experimentally. The time rate of change of the radius was found to be independent of the radius and to vary linearly with the temperature driving force, as predicted theoretically by equation (22). In agreement with theory, equations (23) and (25), the instantaneous and average heat-transfer coefficients were found to be independent of the temperature driving force and inversely proportional to the radius of the lens. However, as exemplified by Fig. 6, the numerical values differ. Quantitatively, this difference is expressed by the ratio of the experimental and theoretical values of m, i.e. $m/m_t \simeq 3{\cdot}5$, yielding that the experimental transfer coefficients are some 3·5 larger than the theoretical ones. It is hoped that a better insight into the actual phenomenon can be gained by scrutinizing the validity of the assumptions inherent in the theoretical derivation as compared with the actual experimental conditions.

Visual observations of isopentane lenses floating on a water surface (Fig. 1), are instructive. When exposed to the free atmosphere, the isopentane–air interface sometimes exhibits a fine, orderly petal shaped, active surface, with some indication that internal circulation takes place. Turbulence of the evaporating lens was also noted [8] at somewhat higher temperature driving forces. The fine wire thermocouple immersed in the lens showed that the temperature of the lens decreased by some 15°C below the normal boiling point during the evaporation into the free atmosphere. A slight decrease of the boiling temperature was also noted under controlled conditions when some air was allowed

into the system, thus reducing the partial pressure of the iso pentane. None of the latter effects were noted when the evaporation process was carried out in a confined atmosphere saturated with isopentane vapor at $(T_\infty - T_0) < 2°C$. However, close observation showed that the exposed surface of the lens (or film) quavered continuously.

The proposed model is based on the assumption of interfacial stability and the absence of Be'nard [10] and Marangoni [11] types of cellular convection. These convective effects [11–15], due to local variation of interfacial tension and density, were expected to be small at the low temperature driving forces which are of practical importance. (Consistent with the small interfacial effects found by Garner [16] at low concentration gradients.) Obviously interfacial effects cannot be completely ignored even at low driving forces and the proposed analysis should be considered as a limiting case of zero convection. It may, therefore, serve only for the lower bound transfer rates, consistent with the experimental evidence.

The instantaneous rate of heat transfer at the liquid–liquid interface was calculated under the assumption of a quasi-steady state condition. This, incidentally, would have been the case, had the lens (or film) been replenished continuously. Indeed, this is not the true physical situation since an unsteady state condition obviously prevails. However, Luchak and Langstroth [17] prove that a quasi-steady state assumption for evaporating spherical drops would affect the calculated evaporation rate by less than 1 per cent, and a similar order or magnitude error may be expected here.

The assumption of a constant evaporation temperature is substantiated by previous investigations of evaporation rates of drops in gaseous media. Soo and Ihring [18] showed that even in the absence of convection, the effect of the initial droplet temperature on the droplet life was insignificant. After a short transient condition the droplet temperature reaches the wet bulb temperature (or the saturated liquid temperature of the system), at which point the droplet temperature becomes uniform and all the heat transferred from the surrounding goes into the latent heat of evaporation [18]. This corresponds to the quasi steady state treated here.

As shown in Fig. 4, the exact time at which evaporation ends is not exactly known. This of course affects the value of the evaporation time t required to evaluate the time-averaged heat-transfer coefficients in equations (25) and (32). Hence, a somewhat arbitrary choice of t was required, and the range of $R_i > R > 0{\cdot}1\, R_i$ used in these equations, seems quite reasonable. Moreover, since the same value of t was used for the theoretical and experimental calculations the absolute value of t would not affect their comparative values.

Figures (5) and (6) demonstrate that convective and interfacial effects are by no means negligible in the present system even at low temperature driving forces. However, some additional factors may have contributed to increase the experimental evaporation rates above the theoretical values. Chief among these is the temperature gradient found in the water phase before each experiment. This was due to natural convection. However, since the experiments were conducted in the absence of mixing (mixing of the water phase was stopped 3 min before each run) this effect was unavoidable. It is estimated that this effect would account for some 30 per cent of the observed difference.

Included in Fig. 6 are curves representing the experimental heat transfer coefficients obtained with pentane drops evaporating while rising freely in a column of water. Curve A represents the average heat-transfer coefficient related to the initial liquid area of the immersed drop whereas curve B represents the same average heat-transfer coefficient, related to the overall instantaneous area of the two-phase drop. The initial volume of the drop is obviously the common denominator in both processes and the double abcissa is scaled to represent identical initial volumes of the liquid. In view of

the convective nature of the latter process, the results are not surprising. Moreover, these results encourage the continued study of evaporating films and stratified layers in convective systems. Work in this direction is presently under way.

ACKNOWLEDGEMENTS

The financial support of the Fohs Foundation enabled the experimental part of this work. The continued support of the National Council for Research and Development into the basic study of direct heat transfer phenomena is thankfully acknowledged.

This paper is based, in part, on the thesis of U. Landau submitted (August 1967) to the Senate of the Technion, Israel Institute of Technology, in partial fullfilment of the requirements for the M.Sc. degree in Chemical Engineering.

REFERENCES

1. S. SIDEMAN, Direct contact heat transfer between immiscible liquids, *Advances in Chemical Engineering* (Edited by T. B. DREW *et al.*) Vol. 6, p. 248. Academic Press, New York (1966).
2. S. SIDEMAN and Y. TAITEL, Direct contact heat transfer with change of phase: evaporation of drops in an immiscible liquid medium, *Int. J. Heat Mass Transfer* **7**, 1273 (1964).
3. S. SIDEMAN and Y. GAT, Direct contact heat transfer with change of phase: spray-column studies of a three-phase heat exchanger, *A.I.Ch.E. Jl* **12**, 296 (1966).
4. S. SIDEMAN, G. HIRSCH and Y. GAT, Direct contact heat transfer with change of phase: effect of the initial dropsize in three phase heat exchangers, *A.I.Ch.E. Jl* **11**, 1081 (1965).
5. M. BENTWICH, Free and forced vibrations of a membrance in contact with air, *Acostica* **12**, 366 (1962).
6. M. BENTWICH, Two dimensional free streamline flow, *Proc. 5th Israeli Conference on Aviation and Astronautics*, p. 82 (1963).
7. H. A. CARLSHAW and J. C. JAEGER, *Conduction of Heat in Solids*, p. 215 Oxford University Press, London (1959).
8. S. SIDEMAN, Photography of drops in liquid media, *Chem. Engng Sci.* **19**, 426 (1964).
9. I. J. LANGMUIR, Oil lenses on water and the nature of monomolecular expanded films, *Chem. Phys.* **1**, 756 (1933).
10. H. BE'NARD, Les toubillons cellulaires dans une nappe liquide transportant de la chaleur par convection en regime permanent. *Ann. Chim. Phys.* **23**, 62 (1901).
11. A. ORELL and J. W. WESTWATER, Spontaneous interfacial cellular convection accompanying mass transfer: ethylene glycol–acetic acid–ethyl acetate, *A.I.Ch.E. Jl* **8**, 350 (1962).
12. F. C. SOMERSCALES and D. DROPKIN, Experimental investigation of the temperature distribution in a horizontal layer of fluid heated from below, *Int. J. Heat Mass Transfer* **9**, 1189 (1966).
13. C. V. STERNLING and L. E. SCRIVEN, Interfacial turbulence: hydrodynamic instability and the Marangoni effect, *A.I.Ch.E. Jl* **5**, 514 (1959).
14. D. A. HAYDON, An investigation of droplet oscillation during mass transfer—I. The conditions necessary, and the source of the energy for the oscillations, *Proc. R. Soc.* A **243**, 483 (1958).
15. T. V. DAVIS and D. A. HAYDON, An investigation of droplet oscillation during mass transfer—II. A dynamical investigation of oscillating spherical droplets, *Proc. R. Soc.* A **243**, 492 (1958).
16. F. H. GARNER, C. W. NUTT and M. F. MOHTADI, pulsation and mass transfer of pendent liquid droplets, *Nature, Lond.* **175**, 603 (1955).
17. G. LUCHAK and G. O. LANGSTROTH, Application of diffusion theory to evaporation from droplets and flat surfaces, *Can. J. Res.* **28**, 547 (1950).
18. S. L. SOO and H. K. IHRING, JR., A study of radius and surface temperature variations of an evaporating liquid droplet in the absence of macroscopic convection, *Proc. Gas Dynamics, Symp. Aero Thermochem.* 35 (1956).

TRANSFERT DE CHALEUR PAR CONTACT DIRECT AVEC CHANGEMENT DE PHASE

Résumé—Le rendement de transport de colennes à pulvérisation et d'autres échangeurs à trois phases, dans lesquels la matière s'évapore (ou se condense) tandis qu'elle est plongée dans la phase non volatile, est diminué par la charge hydrostatique. Cet effet indésirable sur la force motrice thermique peut être surmonté en employant des systèmes dans lesquels la matière qui s'évapore peut flotter sur un liquide non miscible et non volatil. Cette étude est un premier essai pour tester le caractère pratique d'un tel échangeur. Les valeurs limites inférieures des coefficients de transport de chaleur sont obtenues à partir d'une solution de régime quasi-permanent pour une goutte lenticulaire qui s'évapore placée sur un milieu liquide semi-infini au repos.

Le travail expérimental confirme les prédictions théoriques que la vitesse de variation du rayon dè la lentille avec le temps est une constante dépendant de ΔT. Cependant, les vitesses d'évaporation mesurées, d'où les coefficients de transport, sont plus grandes que celles calculées. Ceci nous indique que la convection interfaciale joue un rôle important dans les processus de ce type même pour les forces mortices thermiques faibles. Les coefficients de transport expérimentaux obtenus dans ce travail, se comparent favorablement avec ceux rapportés dans la littérature pour l'évaporation de liquides volatils dans les dispersions.

BERÜHRUNGSWÄRMEÜBERGANG MIT PHASENÄUDERUNG

Zusammenfassung— Der hydrostatische Druck kann einen ungünstigen Einfluss haben auf den Übertragungswirkungsgrad von Rieseltürmen und anderen Dreiphasen-Wärmeübertragern in denen ein Medium, in der nicht-flüchtigen Phase verdampft (oder kondensiert). Dieser unerwünschte Effekt auf das treibende Temperaturgefälle lässt sich sicher dadurch beheben, dass man Anlagen benützt in denen das verdampfende kann. Diese Arbeit bildet einen ersten Versuch die Anwendbarkeit eines solchen Wärmetauschers zu untersuchen. Ziemlich niedrige Grenzwerte für den Wärmeübergangskoeffizienten erhält man aus einer quasistationären Lösung für einen linsenförmigen Tropfen der auf einer halb unendlichen ruhenden Flüssigkeitsschicht verdampft. Experimentelle Untersuchungen bestärken die theoretischen Aussagen, dass die zeitliche Änderung des Linsenradius eine von ΔT unabhängige Konstante ist. Die gemessenen Verdampfungswerte und damit auch die Wärmeübergangskoeffizienten sind grösser als die erechneten. Dies wird als Zeichen dafür gewertet, dass der Wärmeübergang durch die Grenzflächen bei Vorgängen dieser Art sogar bei niedrigen treibendem Temperaturgefälle eine bedeutende Rolle spielt. Die in dieser Arbeit experimentell erhalten Wärmeübergangskoeffizienten stimmen gut mit den Werten der Literature für die Verdampfung von flüchtigen Flüssigkeiten in Dispersionen überein.

Аннотация—Гидростатический напор неблагоприятно влияет на эффективность переноса в распылительных колонках и других трехфазных теплообменниках, где происходит испарение (или конденсация) вещества, погруженного в нелетучую фазу. Это нежелательное влияние на температурный напор можно устранить использованием систем, в которых испаряющееся вещество может течь в несмешивающейся нелетучей жидкости. Данная работа является первой попыткой в осуществлении на практике такого теплообменника. Из решения для случая квазистационарного состояния для испаряющейся линзообразной капли, помещенной в полубесконечную неподвижную жидкую среду, получились заниженные значения коэффициентов теплообмена.

Эксперименты подтверждают теоретический расчет о том, что скорость изменения радиуса линзы во времени есть постоянная зависимость ΔT. Найдено, что измеренные скорости испарения, а следовательно, коэффициенты теплообмена больше расчетных. Это указывает на то, что конвекция на границе раздела играет существенную роль в таких процессах даже при низких температурных напорах. Экспериментально полученные в данной работе коэффициенты теплообмена сравниваются с имеющими в литературе при испарении диспергированных летучих жидкостей.